Multicomponent modelling of cement paste dehydration under different heating rates

Jin Wang, Laurie Lacarriere, Alain Sellier

▶ **To cite this version:**

Jin Wang, Laurie Lacarriere, Alain Sellier. Multicomponent modelling of cement paste dehydration under different heating rates. Materials and structures, 2019, 52 (6), 10.1617/s11527-018-1306-9 . hal-02001210

HAL Id: hal-02001210

https://hal.insa-toulouse.fr/hal-02001210

Submitted on 20 Feb 2019

HAL is a multi-disciplinary open access archive for the deposit and dissemination of scientific research documents, whether they are published or not. The documents may come from teaching and research institutions in France or abroad, or from public or private research centers.

L'archive ouverte pluridisciplinaire **HAL**, est destinée au dépôt et à la diffusion de documents scientifiques de niveau recherche, publiés ou non, émanant des établissements d'enseignement et de recherche français ou étrangers, des laboratoires publics ou privés.

Materials and Structures manuscript No.
(will be inserted by the editor)

Multicomponent modelling of cement paste dehydration under different heating rates

Jin WANG · Laurie LACARRIERE · Alain SELLIER

Received: date / Accepted: date

Abstract The aim of this study is to establish a dehydration model that is able to calculate the water release of cement paste at elevated temperature. The main hydrates in ordinary Portland cement paste (C-S-H, portlandite, aluminates and sulfo-aluminates) were modelled separately and then combined to form the model of the cement paste. In this way, the model is able to predict the dehydration of cement pastes with different compositions without re-fitting. For each hydrate, the dehydration law takes account not only of the maximum quantity of water that can be released at each temperature but also of the kinetics to reach that equilibrium. The model is thus able to reproduce the paste dehydration for any heating rate.
Thermogravimetric tests were carried out with different heating rates to validate

J. Wang
Université de Toulouse, UPS, INSA, LMDC (Laboratoire Matériaux et Durabilité des Constructions)
135 Avenue de Rangueil
31077 Toulouse Cedex 04
France
China construction eighth engineering bureau Co., Ltd
200122, Shanghai
China

L. Lacarriere
Université de Toulouse, UPS, INSA, LMDC (Laboratoire Matériaux et Durabilité des Constructions)
135 Avenue de Rangueil
31077 Toulouse Cedex 04
France
E-mail: laurie.lacarriere@insa-toulouse.fr

A. Sellier
Université de Toulouse, UPS, INSA, LMDC (Laboratoire Matériaux et Durabilité des Constructions)
135 Avenue de Rangueil
31077 Toulouse Cedex 04
France
E-mail: alain.sellier@insa-toulouse.fr

the model in comparison to experimental results from the literature. The results demonstrated the capability of the model in different situations.

Keywords Dehydration · multicomponent modelling · elevated temperature · cement paste · heating rate

1 Introduction

At elevated temperature, cement paste will undergo loss of chemically bound water of the hydrates. This dehydration is of interest when studying the durability and stability of concrete structures in severe environments such as elevated temperatures that can be encountered, for instance, in nuclear confinement structures when there is a severe accident, or in tunnels subjected to fire. Indeed, the paste modification induced by these elevated temperature leads to a loss of mechanical and transfer properties of the concrete. In most cases of structural applications, the dehydration at slightly elevated temperatures is modelled by empirical dehydration law that required to be identifed on a laboratory test performed on the paste used to formulate the concrete or by linear evolution according to temperature supposed to be independent of the cement nature [1,2,3]. However it can be observed in tests with thermogravimetric analysis (TGA) that dehydration is a non-linear phenomenon that depends on the heating rate. These empirical laws, used, for instance, to reproduce the behaviour of a nuclear confinement vessel during a severe accident (inside temperature increasing to 200°C in a matter of minutes), are identified from laboratory tests such as TGA, which are usually performed with a heating rate of 5 K/min. The heating rate used to identify the parameters of such a dehydration law is thus very different from the real heating kinetics (which is linked to the heating source on the surface but may be different at the core because it is also linked to the thermal conductivity) and will have an impact on the dehydration kinetics. Moreover, such empirical laws required a test on the same paste formulation than the one used in the structure and cannot be used as a prediction tool for other concretes. There is thus a need for a model able to predict separately the dehydration of each hydrate of the cement paste with specific kinetics laws adapted to the different mineralogy of hydrates (crystalline or amorphous). Based on previous experience of hydration modelling [4], this study deals with the formulation of such multicomponent dehydration model that could manage the bound water release of each hydrate using intrinsic laws based on mineralogy and stoichiometry considerations.

The effect of the heating rate on dehydration kinetics can be taken into account by introducing a kinetic parameter into the dehydration law, as proposed, for instance, by Zhang [5]. For a well crystallized phase such as calcium hydroxide (CH), all the chemically bound water is released as soon as the temperature that corresponds to the phase equilibrium is reached (with specific kinetics). The dehydration is thus complete even if the temperature is maintained at this value corresponding to the disequilibrium of the phase. In this case, a purely kinetic approach like the one proposed in [5] can be justified. However for amorphous structures like C-S-H (main phase in hydrated cement paste), the mass loss is not linked to a complete dissolution of the hydrate but to a progressive release of the interlayer water depending on the temperature. The most accessible water layers

are thus released at lower temperatures than the most strongly bound water layers. In this case, the dehydration begins at moderate temperature but, if the temperature is maintained at a moderate value, only the most accessible water layers, the ones that are accessible with this energy, are released. The dehydration will thus stop when the water accessible at this temperature has been lost. However, when using a pure kinetic dehydration law, even if the temperature is maintained at a moderate level, the dehydration will continue until all the water has been released. This is due to the fact that progressive dehydration equilibrium with temperature is not considered.

2 Multicomponent dehydration model

The formulation of our model was inspired by the approach proposed by Ferraille [6], which considered both kinetics and equilibrium. However, in order to obtain a model that could easily be used for different cements without any refitting to avoid new characterization tests, in our approach the kinetics of water mass loss due to dehydration is calculated from the mass loss kinetics for each separate hydrate j of the cement paste using eq. 1.

$$\dot{w}_{dehyd} = -\sum_{j} Q_j^W \cdot \dot{\xi}^j \tag{1}$$

where:

- ξ^j is the dehydration degree for hydrate j ;
- Q_j^W is the chemically bound water contained in the hydrate j before the dehydration.

This quantity of chemically bound water Q_j^W contained in the hydrate j at the beginning of dehydration ($t_{0\,des}$) can be calculated from the hydration degree of the anhydrous phase i for which the reaction produces or consumes hydrate j and from stoichiometric consideration [4,7]. For instance, for Portland cements, only clinker is considered, so $i = \{clinker\}$. In this case, and for cement with low sulfure content, the produced hydrates are CH, C-S-H and AFm, so the calculation of Q^W would have to be performed for these 3 hydrates.

$$Q_j^W = \int_0^{t_{0\,dehyd}} \sum_i \left(H_{Hyd_j} \cdot \frac{\partial Hyd_j}{\partial \alpha_i} \cdot \frac{\partial \alpha_i}{\partial t} \right) \cdot dt \tag{2}$$

where:

- α_i is the hydration degree of anhydrous phase i;
- H_{Hyd_j} is the mass of water in 1 mole of hydrate j;
- $\frac{\partial Hyd_j}{\partial \alpha}$ is the molar quantity of hydrate j produced (> 0) or consumed (< 0) by the reaction of 1 unit of mass of the anhydrous phase i (calculated from stoichiometric considerations [7]).

The dehydration kinetics for each hydrate is determined at each time step by considering the difference between the equilibrium and actual degrees of dehydration and a characteristic time managing the kinetics (equation 3). The kinetics

is thermoactivated in order to consider the faster dehydrations observed at high temperatures (for instance, as shown for portlandite in [5]).

$$\dot{\xi^j} = \underbrace{H(T - T^j{}_o)}_{\text{onset effect}} \cdot \underbrace{\left(\xi^j_{eq}(T) - \xi^j\right)}_{\text{disequilibrium}} \underbrace{\frac{1}{\tau^j} \exp\left(-\frac{E^j_a}{R}\left(\frac{1}{T} - \frac{1}{T^j{}_o}\right)\right)}_{\text{kinetic}} \tag{3}$$

where:

- $\xi^j_{eq}(T)$ is the final dehydration degree at a given temperature;
- $H(T - T^j{}_o)$ is the Heaviside function;
- $T^j{}_o$ is the temperature from which the hydrate j begins to dehydrate (onset temperature) . This temperature is also used as reference temperature for the thermoactivation of dehydration. Temperatures T and $T^j{}_o$ must be given in [K];
- τ^j is the characteristic time associated with hydrate j;
- E^j_a is the activation energy associated with hydrate j.

The equilibrium degree of dehydration ($\xi^j_{eq}(T)$ in equation 3) depends on the crystalline structure of the hydrate concerned. For a well crystallized hydrate (such as CH), it is equal to 1, characterizing the complete dissolution of the hydrate. In contrast, for amorphous hydrates (such as C-S-H), the equilibrium dehydration degree is a function depending on temperature and thus characterizing a dependence of interlayer water loss on the temperature.

The aim of this work is to determine the equilibrium degree (ξ^j_{eq}) and the constants managing the kinetics (τ^j) and its dependence on temperature (E^j_a) for each hydrate of a cement paste. These parameters are then considered as intrinsic because they depend only on the nature of the hydrate,and not on its quantity, for example.

3 Determination of parameters of dehydration law for each hydrate

In this section the parameters of the dehydration laws for each hydrate are determined by minimizing the difference between theoretical and experimental results issued from literature. For each hydrate, the theoretical dehydration curves are obtained integrating equation 3 using a finite difference method with explicit scheme in which the time step time step is controlled to limit the variation of $\dot{\xi^j}$ to 10^{-4}.

3.1 Dehydration of CH

Due to its crystalline structure, the equilibrium dehydration degree of calcium hydroxide (ξ^{CH}_{eq} in eq. 3) is equal to 1. The progressive mass loss when temperature increases is only managed by the kinetic parameters, which have to be identified (τ^{CH} and E^{CH}_a in eq. 3).

Zelic [8] performed TGA tests on specimens of pure CH at different heating rates in order to highlight these kinetic phenomena. Those tests thus allowed the kinetic parameters of our model to be identified. The values found were $\tau^{CH} = 17.4$ h and $E^{CH}_a = 158$ kJ/mol. E_a is considered equal to the average of the values that can be identified with the classical method for determination of activation energies

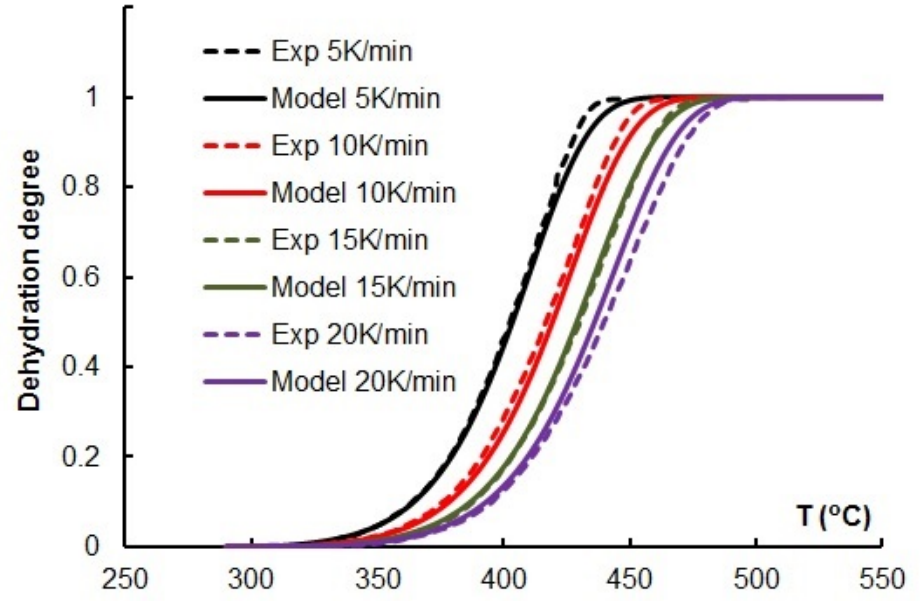

Fig. 1: Dehydration of CH (experimental results from [8])

used for instance in [5]. The comparison between the model and Zelic's results is illustrated in Fig. 1. It must be noticed that only the kinetic parameters can be fitted on these results on pure CH. The onset temperature (from which the decomposition begins) observed in pure CH is indeed lower than the one observed for CH in cement paste (as shown by the authors [8]). The onset temperature for CH in cement paste (presented on table 1) is fixed to 375°C according to the observation of [8].

3.2 Dehydration of tricalcium aluminate hexahydrate

Like CH, tricalcium aluminate hexahydrate (C_3AH_6, written TCA) also has a crystallized structure that gives it an equilibrium dehydration degree (ξ_{eq}^{TCA} in eq. 3) of 1. The progressive mass loss when temperature increases is managed only by the kinetic parameters that have to be identified (τ^{TCA} and E_a^{TCA} in eq. 3).

From Rivas-Mercury's TGA-DSC results [9], it can be noted that tricalcium aluminate hexahydrate (TCA) loses most of its water above 200°C . Horváth proposed that the dehydroxylation of TCA occurred in the 260-400°C temperature range and that the activation energy of the reaction was 85.4 kJ/mol [10]. S.K. Das reported that the peak of the differential scanning calorimetry test (DSC) in the process of dehydration occurred at 310°C and the activation energy was found to be 35.58 kJ/mol[11]. Rivas-Mercury performed the TGA test and neutron thermodiffractometry and claims that the whole dehydration process consisted of two stages[9]. Nevertheless, most of the mass loss (around 80%) took place in the 200-300°C temperature range. It was mentioned that the TGA test might have been

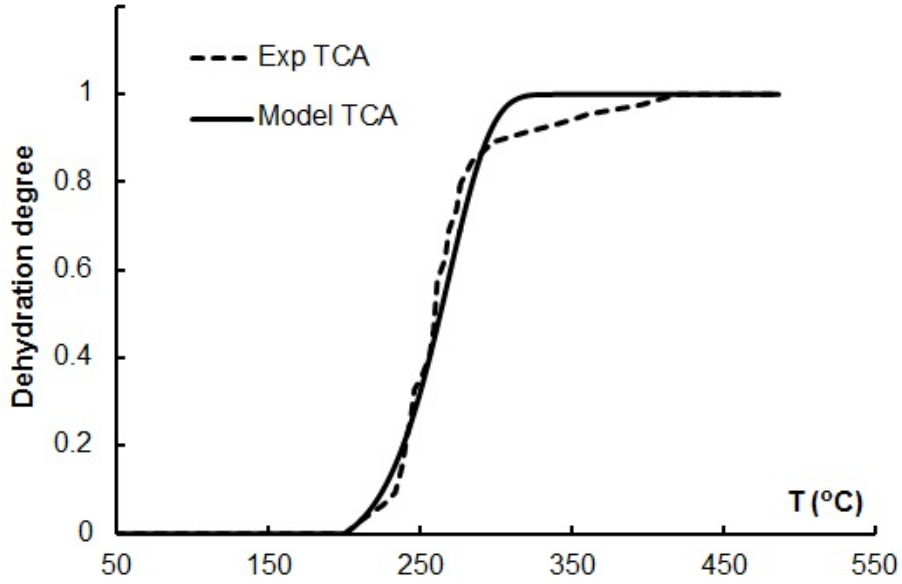

Fig. 2: Dehydration of TCA (C_3AH_6) (experimental results from [9])

influenced by the presence of CH introduced during the sample preparation. In addition, a comparison with the experimental results mentioned above suggests that the mass loss before 200°C was probably not due to dehydration of TCA. Hence, a simplification was made by considering that the dehydration of the TCA started from 200°C and that only the mass loss between 200°C and 300°C corresponded to the dehydration of calcium aluminate.

Results from Horváth [10] identify the activation energy of dehydration $E_a^{TCA} = 85.4$ kJ/mol. Using this value with Rivas-Mercurys results [9] allows the characteristic time to be identified. The value adopted here is $\tau^{TCA} = 3.3$ h and a comparison of the model with Rivas-Mercury's results is illustrated in Fig. 2.

3.3 Dehydration of monosulfoaluminate

The water in the monosulfate ($C_4A\bar{S}H_{12}$, written AFm) is usually considered to be made up of two types: the interlayer water and the bound water [12,13,14]. The water loss of AFm with temperature occurs through two different mechanisms. Leisinger [13] showed that the interlayer water was released progressively from around 40°C . This can be explained, as for C-S-H, by the fact that, when the temperature increases, the associated energy allows a new water layer to be extracted. At higher temperature, when this interlayer water has all been released, AFm exhibits a crystalline structure which is shown by a peak in the DSC curve centred around 300°C [13]. A quantitative analysis of Leinsingers results shows that the crystalline structure contains 6 moles of water. In the study exposed in the present paper, only the release of water due to temperature increase alone is

considered. The interlayer water that can be released by dehydration corresponds to around 6 mol/mol of AFm [12,13,14].

The degree of dehydration of monosulfate can thus be calculated as a weighted combination of the dehydration degree corresponding to the crystalline part of AFm ($\dot{\xi}^{\mathrm{AFm}_{cryst}}$) and that corresponding to the interlayer water which is not able to move by a decrease of relative humidity alone ($\dot{\xi}^{\mathrm{AFm}_{layer}}$) (eq. 4). AFm contains 12 moles of water per mole of AFm before dehydration and, as the water content in each part of AFm is equal to 6 moles per mole of AFm, the weighted coefficient is equal to 6/12=0.5.

$$\dot{\xi}^{\mathrm{AFm}} = 0.5 \cdot \dot{\xi}^{\mathrm{AFm}_{layer}} + 0.5 \cdot \dot{\xi}^{\mathrm{AFm}_{cryst}} \tag{4}$$

The loss of interlayer water is modelled using an equilibrium degree of dehydration ($\xi_{eq}^{\mathrm{AFm}_{layer}}$ in eq. 3) that depends on the temperature as proposed in equation 5 (to reproduce progressive loss of water). As this interlayer water does not correspond to a crystalline structure the dehydration process does not need the temperature to reach a specific value (corresponding to the crystalline structure destabilisation). The dehydration process is thus considered to begin from the reference temperature of 40°C but with a kinetic depending on temperature (lower kinetic for low temperatures).

$$\xi_{eq}^{\mathrm{AFm}_{layer}} = 1 - \exp\left(-0.06\left(T - {T_0}^{\mathrm{AFm}_{layer}}\right)^{0.8}\right) \tag{5}$$

This equation is represented in Fig. 4 and is compared with the evolution of the equilibrium degrees of other hydrates. The parameters of this equation 5, together with the constants managing kinetics and its dependence on temperature (eq. 3), are identified using literature results for temperatures below 150°C which is the onset temperature associated with the loss of the structural water (AFm_{cryst}). The values adopted for the interlayer water are $\tau^{\mathrm{AFm}_{layer}} = 0.2$ h and $E_a^{\mathrm{AFm}_{layer}} = 10$ kJ/mol and the comparison between the model and the experimental results is illustrated in Fig. 3 (temperature below 150°C).

As for other crystalline structures, the loss of structural water (decomposition of $C_3A\bar{S}H_6$) is associated with an equilibrium degree of dehydration ($\xi_{eq}^{\mathrm{AFm}_{cryst}}$ in eq. 3) equal to 1 and to an onset temperature below which the crystalline structure is stable (equal to 150°C for AFm). The constants managing the kinetics and its dependence on temperature (eq. 3) are identified using literature results above 150°C . The values adopted are $\tau^{\mathrm{AFm}_{cryst}} = 0.5$ h and $E_a^{\mathrm{AFm}_{cryst}} = 20$ kJ/mol, and the comparison between the model and experimental results is illustrated in fig. 3.

3.4 Dehydration of C-S-H

Based on the work of Jennings [15], the bound water of C-S-H, which will be managed by the dehydration model, is considered to correspond to an H/S ratio of 1.4 whatever the C/S ratio. The complementary water is considered as free water and is managed by the hydric equilibrium and the water retention curves. It means that the differences in water content observed on C-S-H with different C/S ratios is only due to free water which can be removed without heating (for

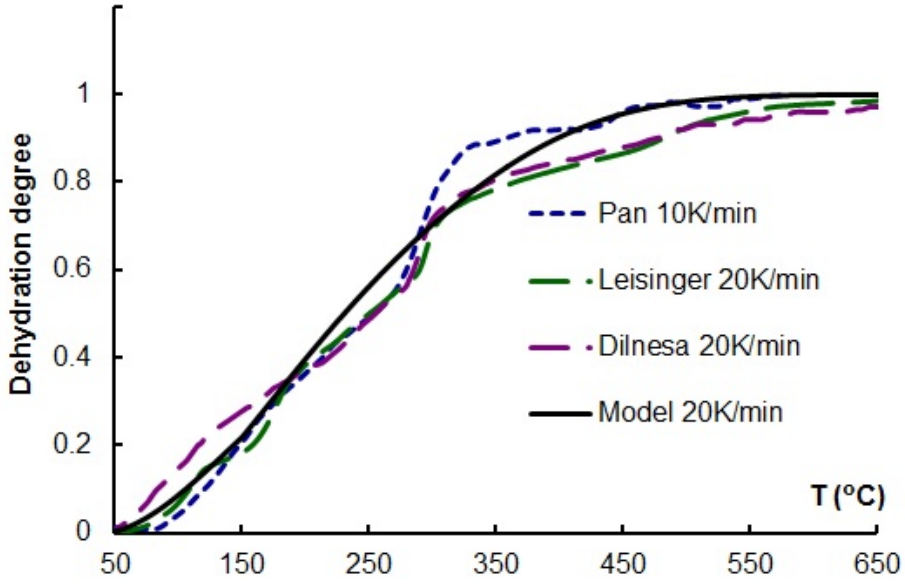

Fig. 3: Dehydration of AFm (experimental results from [14,13,12])

instance by decreasing the relative humidity). It is confirmed on fig. 4 where it can be seen that the water loss from 100°C to 450°C is similar for C-S-H with different C/S ratios.

Due to their amorphous structure with layers, the loss of bound water from C-S-H, even when equilibrium is reached, depends on the temperature which corresponds to the energy level of a specific part of the interlayer water. The equilibrium dehydration degree (ξ_{eq}^{CSH} in eq. 3) adopted in this model is thus, as for the interlayer water of AFm, an exponential function (eq. 6), even though the parameters of this function are expected to differ from that of AFm (interlayer water in C-S-H is bound by the hydrogen bond and, as in AFm, it is connected with Ca^{2+}). This equation is represented in Fig. 4, where it is compared with the evolution of the equilibrium degrees of other hydrates. As for the interlayer water in AFm, the bound water in C-S-H does not correspond to a crystalline structure, so the dehydration process does not need the temperature to reach a specific value to start. The dehydration process is thus considered to begin from the reference temperature of 40°C but with a kinetic depending on temperature (very slow kinetic for temperature below 100°C .

$$\xi_{eq}^{CSH} = 1 - \exp\left(-0.01\left(T - {T_0}^{CSH}\right)^{0.9}\right) \tag{6}$$

The parameters of this equation 6 as well as the constants managing kinetics and its dependence on temperature (eq. 3) were identified using literature results by Rodriguez [16] and Foley [17]. Below 100°C and depending of the sample preparation, some free water (the one able to move with only a decrease of relative humidity and corresponding to $H/S > 1.4$) can be remaining in the samples. That's why, to identify the parameter of the dehydration law, only the loss of

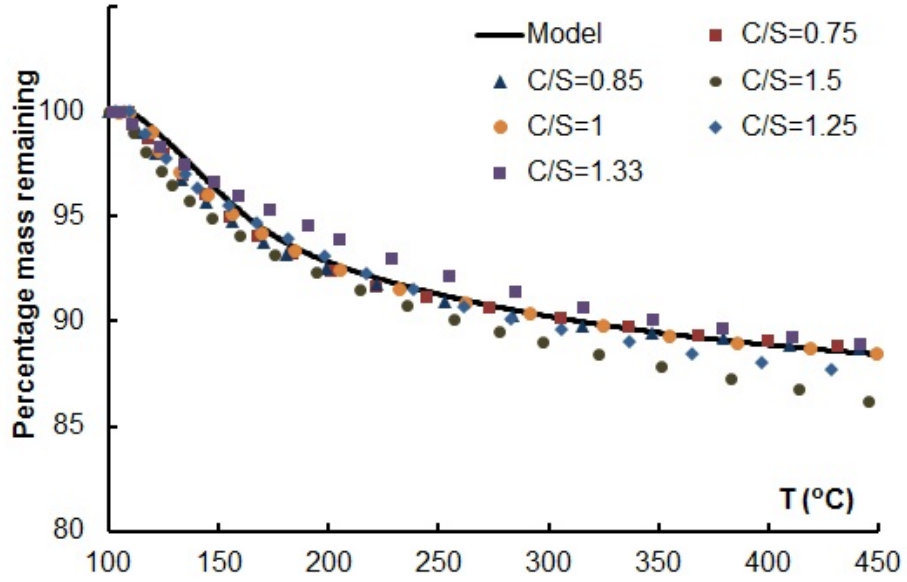

Fig. 4: Identification of dehydration parameters for $C_xSH_{1.4}$ (experimental mass loss after 100°C calculated from the results of [16])

mass after 100°C is used in Fig. 4. The values adopted are $\tau^{CSH} = 1$ h and $E_a^{CSH} = 34$ kJ/mol, and the comparison of the model with Rodriguez's results is illustrated in Fig. 4. It can bee seen on Fig. 7 for instance, that the low kinetic for low temperatures leads to quite no mass loss below 100°C for a heating rate equal to 10K/min (usual value for TGA tests)

3.5 Summary of the dehydration law parameters

The results of the identification are summarized for the different hydrates in Table 1, which gives the onset temperature, the characteristic time and the activation energy managing the kinetic part of the dehydration laws.

Table 1: Dehydration law's parameters for each hydrate

	T_o^j (°C)	τ^j (h)	E_a^j (kJ/mol)
CH	375	17.4	158.53
TCA	200	3.3	85.4
AFm_{layer}	40	0.2	10
AFm_{cryst}	150	0.5	20
$C_xSH_{1.4}$	40	1.	34

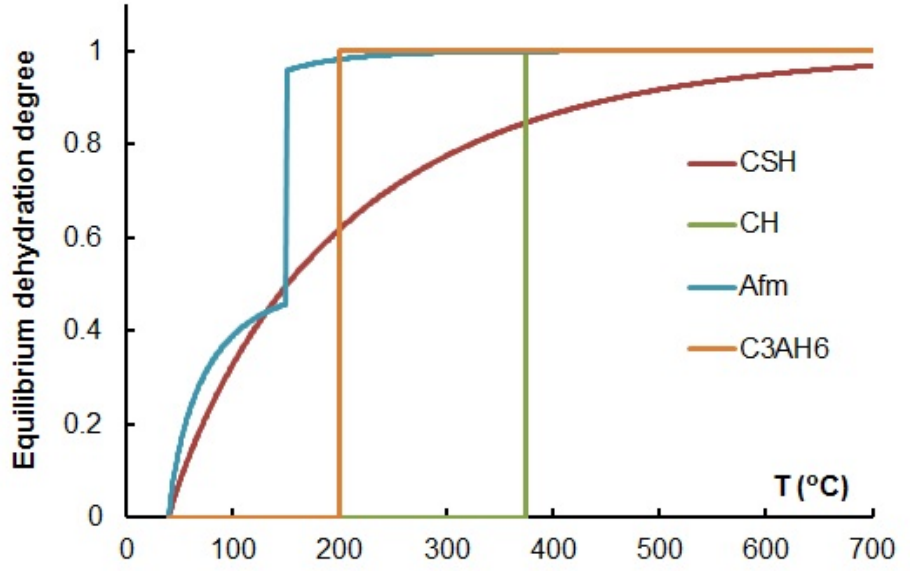

Fig. 5: Equilibrium degree of dehydration for the different hydrates

Table 2 presents the functions of equilibrium degree for each hydrate, with the parameters identified using the literature results presented earlier. These functions are illustrated in Fig. 5 for temperatures between 50°C and 700°C. It can be observed that, in a cement paste, below 200°C the loss of water will be due only to the dehydration of C-S-H and AFm.

Table 2: Equilibrium degree of dehydration for each hydrate

	ξ_{eq}^{j}
CH	1
TCA	1
AFm_{layer}	$1-\exp\left(-0.06\,(T-40°\mathrm{C}\,)^{0.8}\right)$
AFm_{cryst}	1
$C_xSH_{1.4}$	$1-\exp\left(-0.01\,(T-40°\mathrm{C}\,)^{0.9}\right)$

4 Application to the simulation of experimental results on cement pastes and parametric study

In order to evaluate the ability of the model to reproduce (without any refitting) the dehydration of cement pastes with different heating rates, 2 TGA tests were performed on a paste cast with W/C=0.5, using CEM I 52.5 cement. The specimen had been cured in sealed cylindrical plastic tubes (ϕ30 mm × 60 mm) at 20°C for

60 days. To remove the free water, the specimens were soaked in liquid nitrogen for 5 minutes immediately after being taken out of the tube, and then dried with lyophilization at -50°C using the Labconco Free Zone 4.5 lyophilizer for 48h. After drying, the samples were ground until all of them passed the 80μm sieve before the TGA test. The TGA was run on the STA 449 F3 analyser manufactured by Netzsch. The temperature range for the test was 40-800°C at heating rates of 5 K/min and 10 K/min.

Two other cement pastes taken from the literature were tested. They were selected among several available data because, in these works, all the experimental conditions (cement composition, heating rate, pre-drying process, etc.) were given. Morandeau [18] tested an ordinary paste with a W/C ratio of 0.45 and Alarcon-Ruiz [19] performed TGA on a paste with a low W/C ratio (0.33) and with a cement containing more Al_2O_3. The compositions of the cements used in the experiments are listed in Table 3. The heating rate was 10 K/min for Morandeau and 5 K/min for Alarcon.

The chemical compositions of the 3 cements tested are given in Table 3.

Table 3: Composition of the cement (%w.t. for oxyde and mass ratio for W/C)

	LMDC	[18]	[19]
SiO_2	20.6	22.12	19.45
Al_2O_3	4.5	3.69	4.8
Fe_2O_3	2.3	4.	1.75
CaO	63.2	65.03	59
SO_3	3.3	2.94	2.95
W/C	0.5	0.45	0.33

As the model was developed as a multicomponent model, the dehydration of different cement pastes should be predicted without any refitting, with only the chemical composition of cement and water to cement ratio as data. Indeed, the water content per unit volume of cement pastes, before the beginging of the dehydration test, can be calculated using the stoichiometry for each hydrate and the hydrate mole number computed by the hydration model developed previously in our laboratory [4,7], only from the oxide content in cement and the water to cement ratio. This quantity of water content of each kind of hydrate (in kg/m^3 of paste) at the end of the curing period is given in Table 4 for the paste tested in our laboratory and for the 2 pastes drawn from the literature.

For the three studies (LMDC and [18,19]) the pastes were dried before TGA in order to eliminate free capillary water, using techniques that also released part of the interlayer water of AFm (D-drying and 105°C oven drying), this pre-release of 4 moles of H per mole of AFm thus had to be deducted from the water evaluated by hydration. The quantity of water lost due to pre-drying (that should be subtracted from the water content in each hydrate before applying the dehydration model) is also given in Table 4.

The results of the TGA tests are compared to the predictions of the dehydration model, with the parameters identified from the literature results for each hydrate and recalled in Table 1. The results are presented in terms of percentage of mass of bound water remaining in the paste (as a percentage). This remaining bound

Table 4: Water content of each hydrate in cement paste (kg per 1 m^3 cement paste)

	LMDC	[18]	[19]
CH	54.43	55.1	60.76
AFm	86.65	82.2	97.64
TCA	18.15	27.39	28.0
$C_{1.7}SH_{1.4}$	90.16	103.07	107.30
loss by pre-drying	28.88	27.4	32.50

water ($\%m_{W\,bond}$) is calculated from the mass of the specimen tested (m_{spe}) as given in equation 7 (supposing that the mass obtained at 700°C corresponds to the mass of the solid to avoid taking into account the effect of decomposition of carbonates). In the tests performed at LMDC, as we want to decouple the effect of dehydration and carbonation, a specific care was taken to avoid any carbonation of the sample during the cure and preparation. No loss of mass corresponding to decomposition of carbonate (that should be identified in TGA-DSC test with the measurement of CO_2 release) was observed. In the two litterature tests used to evaluate the prediction capability of the model [18,19], some carbonation was observed. In this first study the hydration model used to predict the initial state of the hydrated paste, before TGA test, is not coupled with a carbonation model. Therefore some differences are expected between the model prediction and the results.

$$\%m_{W\,bond}(T) = \frac{m_{spe}(T) - m_{spe}(700°\mathrm{C})}{m_{spe}(100°\mathrm{C}) - m_{spe}(700°\mathrm{C})} \tag{7}$$

The dehydration model was applied without any re-fitting. The model and test results obtained for 3 different pastes and 2 different heating rates are compared in Figures 6, 7, 8 and 9.

It can be seen that these tests are globally well reproduced by the model for both heating rates (comparison with LMDC results) and for the three different pastes (different W/C ratios and different ordinary cements). The slight difference between model prediction and experimental results for the tests presented in [18, 19] may be explained by the partial carbonation of the paste before the dehydration test (carbonation identified by the authors from the analysis of the TGA test). The carbonation of some hydrates in the specimen during the cure can lead to two sources of misprediction of the model. First, the initial quantity of bound water content at the beginning of the dehydration test can be slightly overestimated because the hydration model that calculated the composition of the hydrated paste does not take into account the conversion of some hydrates into carbonates (which releases some bound water). This could be improved by coupling the hydration and dehydration models with a carbonation model. Then, as the mass of the specimen at 700°C includes the mass of carbonates, the calculation of the bound water as exposed in equation 7 is not exactly made on the same basis.

The model is then tested to illustrate the effect of much broader variation of heating rates such as large heating rates (50K/min) which can be quite representative of fire exposition near the exposed surface and a theoretical extremely slow heating rate which allows to represent the equilibrium degree of dehydration at each temperature (figure 10). It must me noticed that, as the identification of the

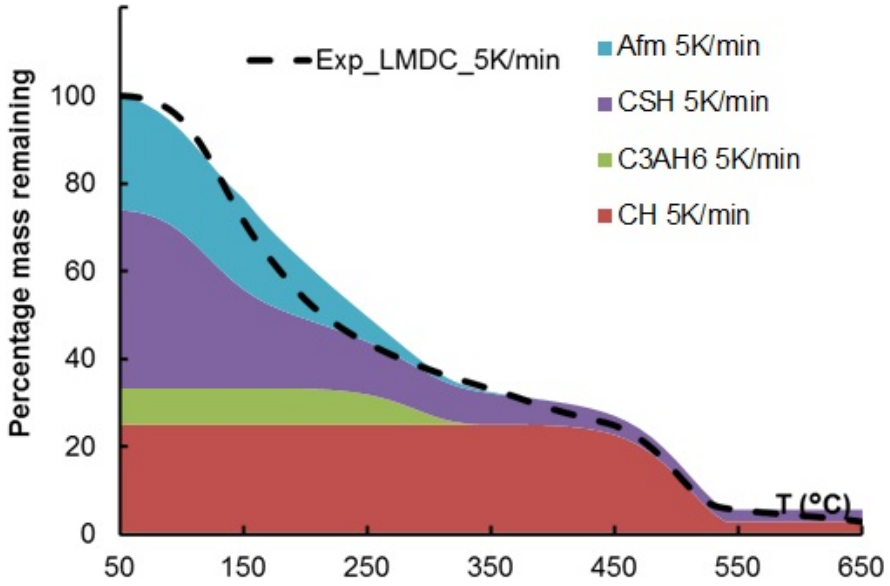

Fig. 6: Comparison with LMDC TGA test under 5K/min

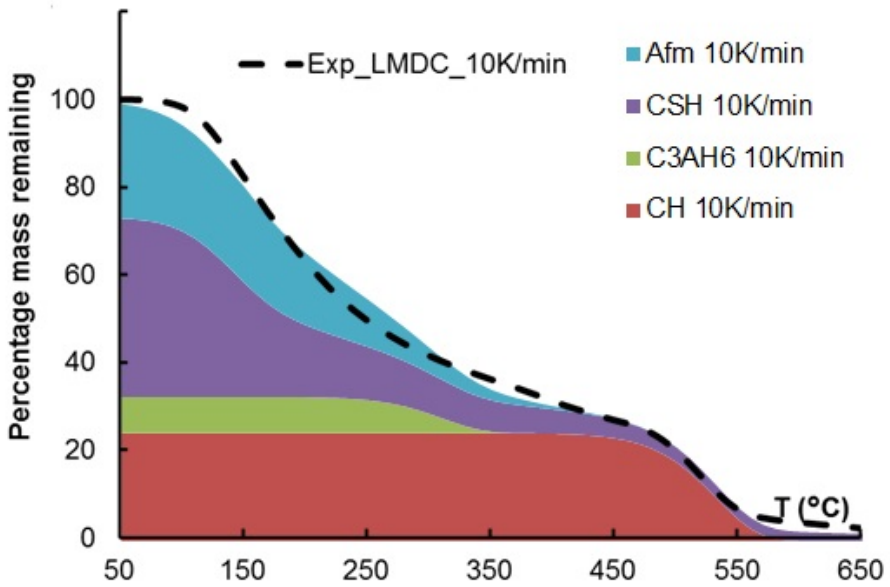

Fig. 7: Comparison with LMDC TGA test under 10K/min

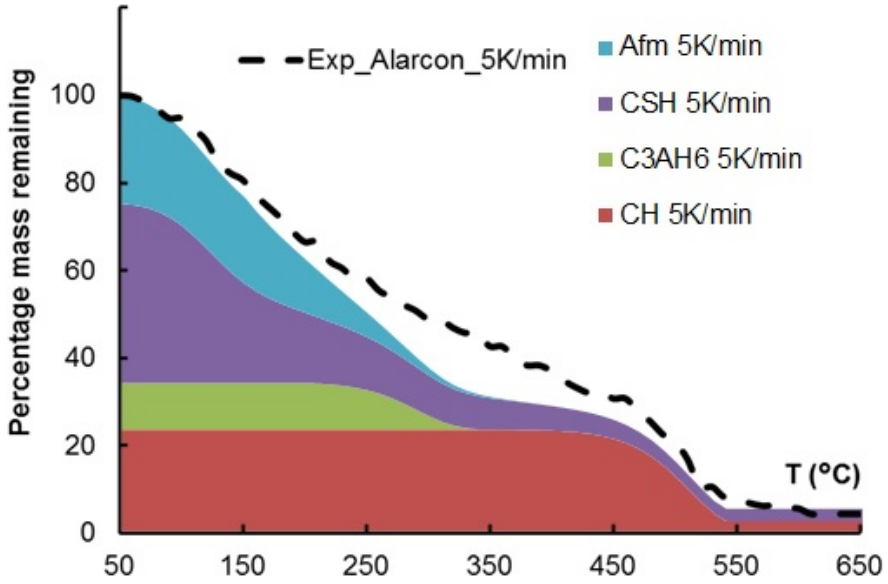

Fig. 8: Comparison between the modeling results and the experiment in[19]

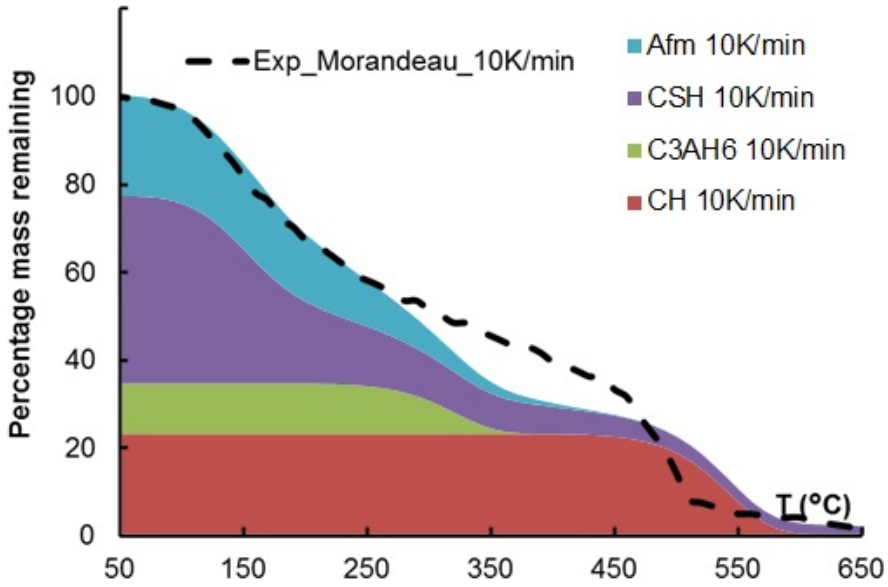

Fig. 9: Comparison between the modeling results and the experiment in[18]

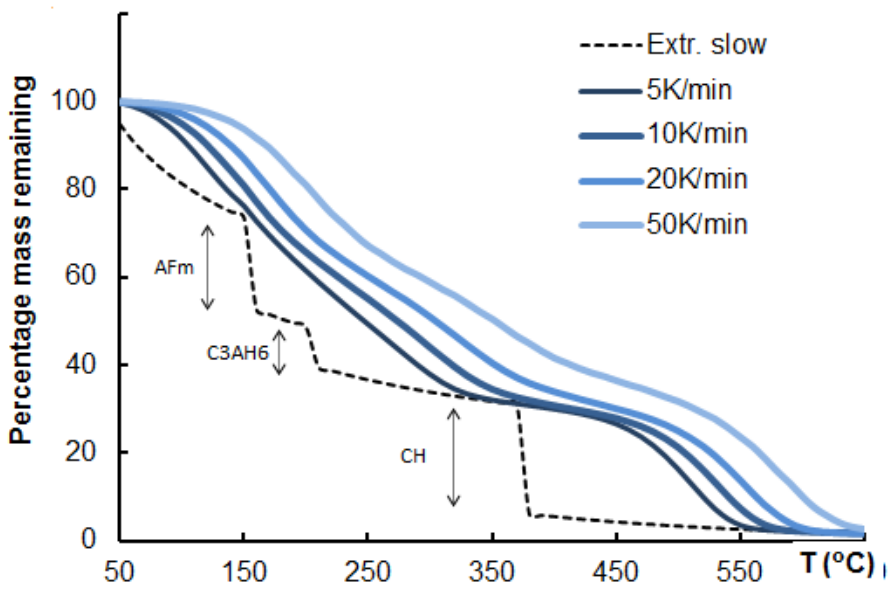

Fig. 10: Parametric study for a cement paste subjected to different heating rates

model's parameters was made for heating rate of 5 or 10K/min, the extrapolation of the model prediction to these much broader variation of heating rates remains theoretical and should be verified with experimental devices allowing such heating configurations. It can be noticed that for heating rates not very fast (5 and 10K/min), the bound water remaining around 400°C corresponds to the one predicted if the equilibrium is reached, that is to say that C-S-H and aluminates lost quite all their bound water before CH decomposition. On the contrary for high heating rates some water remains in these phases before CH decomposition and the profile of the water loss is quite linear according to temperature between 150 and 550°C .

The model is also tested to simulate the effect of a very different cement composition, to illustrate the possible applicability of the model to blended cements in the future. Figure 11 presents the results of dehydration for an ordinary Portland cement and for a cement with a low calcium content which induces that the hydrated paste contains almost no CH.

5 Conclusion

The multicomponent dehydration model for cement paste was established on the basis of the dehydration model for each hydrate in the cement paste. The hydrates taken into account in this study were C-S-H, CH, TCA and AFm.
The model contains both equilibrium and kinetic parts, and can be applied on cement pastes having different compositions without the need to re-fit the parameters. Dehydration models for CH, AFm, TCA and C-S-H were identified from experiments on pure hydrates reported in the literature, in order to ensure that

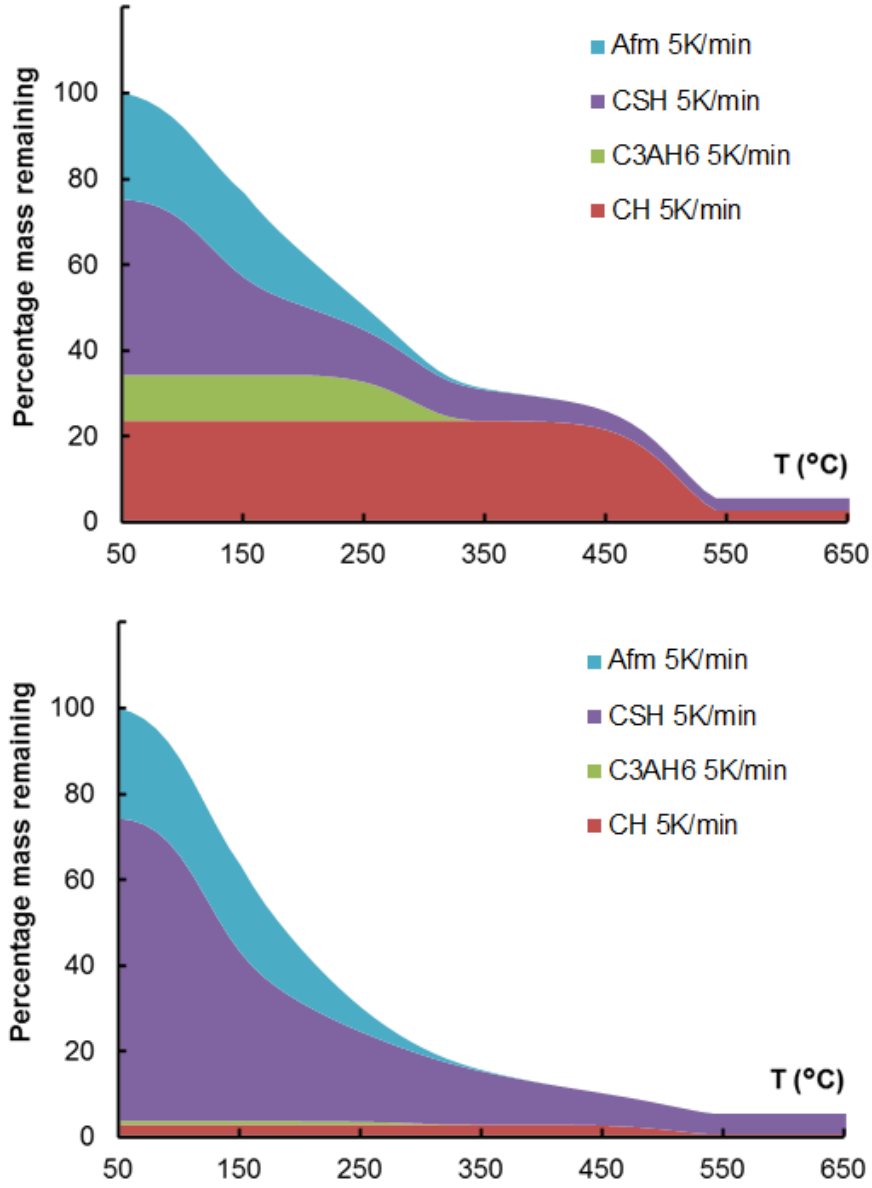

Fig. 11: Prediction of the dehydration of a portland cement and a "low calcium" cement for a heating rate of 5K/min

the model was able to predict the dehydration of every Portland cement paste without refitting, based only on the composition of the paste (quantity of the different hydrates in the hydrated paste), which can be obtained using a previously developed hydration model.
The model was compared with experiments run at different heating rates and with different compositions of cement. It showed its good ability to predict the dehydration process of Portland cement paste between 100 and 650°C . A coupling with ageing model (carbonation for instance) can be envisioned in the future works before extending this multicomponent dehydration model to the prediction of the effect of dehydration on the mechanical properties.

6 Compliance with Ethical Standards:

Funding: This study was funded by the Chinese Scholarship Council (CSC) through Jin Wang's thesis grant and by the French National Research Agency (ANR-PIA) under the MACENA research program 11-RSNR-0012 (Control of nuclear vessel in accident conditions).
Conflict of Interest: The authors declare that they have no conflict of interest.

References

1. B. Bary, G. Ranc, S. Durand, O. Carpentier, A coupled thermo-hydro-mechanical-damage model for concrete subjected to moderate temperatures, International journal of heat and mass transfer **51**(11), 2847 (2008)
2. G. Ranc, J. Sercombe, S. Rodrigues, Comportement haute temprature du bton de structure: Impact de la fissuration sur les transferts hydriques, Revue Franaise de Gnie Civil **7**(4), 397 (2003)
3. D. Gawin, F. Pesavento, An Overview of Modeling Cement Based Materials at Elevated Temperatures with Mechanics of Multi-Phase Porous Media, Fire Technology **48**(3), 753 (2012)
4. L. Buffo-Lacarrire, A. Sellier, G. Escadeillas, A. Turatsinze, Multiphasic finite element modeling of concrete hydration, Cement and Concrete Research **37**(2), 131 (2007)
5. Q. Zhang, G. Ye, Dehydration kinetics of Portland cement paste at high temperature, Journal of Thermal Analysis and Calorimetry **110**(1), 153 (2012)
6. A. Feraille Fresnet, Le role de l'eau dans le comportement haute temprature des btons. Ph.D. thesis, ENPC (2000)
7. B. Kolani, L. Buffo-Lacarrire, A. Sellier, G. Escadeillas, L. Boutillon, L. Linger, Hydration of slag-blended cements, Cement and Concrete Composites **34**(9), 1009 (2012)
8. L.U. Jelica Zelic, D. Jozic, in *The First International Proficiency Testing Conference* (2007)
9. J. Rivas-Mercury, P. Pena, A. de Aza, X. Turrillas, Dehydration of ca3al2(sio4)4(3-y) (0< y< 0.176) studied by neutron thermodiffractometry, Journal of the European Ceramic Society **28**(9), 1737 (2008)
10. I. Horvath, I. Proks, I. Nerad, Activation energies of the thermal decompositions of $\mathrmC_3ah_6$ AND $\mathrmC_3ad_6$ by the isothermal TG method, Journal of thermal analysis **12**(1), 105 (1977)
11. S.K. Das, A. Mitra, P.D. Poddar, Thermal analysis of hydrated calcium aluminates, Journal of thermal analysis **47**(3), 765 (1996)
12. B.Z. Dilnesa, B. Lothenbach, G. Renaudin, A. Wichser, E. Wieland, Stability of Monosulfate in the Presence of Iron, Journal of the American Ceramic Society **95**(10), 3305 (2012)
13. S.M. Leisinger, B. Lothenbach, G. Le Saout, C.A. Johnson, Thermodynamic modeling of solid solutions between monosulfate and monochromate, Cement and Concrete Research **42**(1), 158 (2012)

14. Z.h. Pan Guoyao, Mao Ruoqing, Research of dehydrated calcium sulphoaluminate hydrates (afm) and its hydration, Journal of Wuhan University of Technology **19**(3), 28 (1997)
15. H.M. Jennings, A model for the microstructure of calcium silicate hydrate in cement paste, Cement and Concrete Research **30**(1), 101 (2000)
16. E. Tajuelo Rodriguez, K. Garbev, D. Merz, L. Black, I.G. Richardson, Thermal stability of C-S-H phases and applicability of Richardson and Groves' and Richardson C-(A)-S-H(I) models to synthetic C-S-H, Cement and Concrete Research **93**, 45 (2017)
17. E.M. Foley, J.J. Kim, M.M.R. Taha, Synthesis and nano-mechanical characterization of calcium-silicate-hydrate C-S-H made with 1.5 C/S mixture, Cement and Concrete Research **42**(9), 1225 (2012)
18. A. Morandeau, M. Thiery, P. Dangla, Investigation of the carbonation mechanism of ch and csh in terms of kinetics, microstructure changes and moisture properties, Cement and Concrete Research **56**, 153 (2014)
19. L. Alarcon-Ruiz, G. Platret, E. Massieu, A. Ehrlacher, The use of thermal analysis in assessing the effect of temperature on a cement paste, Cement and Concrete Research **35**(3), 609 (2005)